agreement is apparent both for the degree of scattering at the relevant part of the solar cycle and for the slope of the lines. To illustrate further the solar cycle variation, the inset to Figure 3 shows our values for the radial scattering angle at 12 $R_\odot$ compared to those of other authors[3, 4] over the past 18 years. It is seen that the degree of scattering shows good agreement with the smoothed sunspot numbers for these years.

Lines of best fit were also calculated for the radial scattering values giving a mean slope of −1.6 for the three years. This value may be compared to the slopes −2 and −3, calculated for the tangential broadening in 1969–70 and 1971 respectively. The different radial variations of radial and tangential scattering suggest that the axial ratio of the scattering irregularities may increase close to the Sun.

The results above have been obtained by assuming a tangentially aligned image, and in fact the variation of the major axis from the tangential direction was found to be random with a rms deviation of $\sim 5°$.

We have presented a brief outline of three years of observations of the Crab Nebula during its near-occultation by the Sun. The scattering data agree well with results of other authors for previous years and extends the amount of information which can be obtained from angular broadening observations. The interpretation of the results in terms of various scattering models and a discussion of the variation of axial ratio of the plasma irregularities will be given in the following paper.

It is a pleasure to extend our thanks to the CSIRO, Division of Radiophysics for providing observing facilities on the Radioheliograph. One of us (R.G.B.) acknowledges the support of a Commonwealth Postgraduate Award.

[1] Harries, J. R., Blesing, R. G. and Dennison, P. A., *Proc. ASA*, **1**, 319 (1970).
[2] Wild, J. P. *et al.*, *Proc. IREE Aust.*, **28**, No. 9 (1967).
[3] Okoye, S. E. and Hewish, A., *MNRAS*, **137**, 287 (1967).
[4] Matheson, D. N. and Little, L. T., *Nature*, **234**, 29 (1971).

Coronal Broadening of the Crab Nebula 1969-71

Interpretation

P. A. Dennison and R. G. Blesing
Department of Physics, University of Adelaide

In the preceding paper,[1] observations of the coronal broadening of the Crab Nebula during 1969-71 were described. The basic parameters, radial and tangential broadening, and their relation to previous work were discussed. Whereas previous observations have utilized two or three interferometers only, so that the degree of broadening along any particular axis could only be obtained under the assumption of a particular form (e.g. Gaussian) for the angular power spectrum, the present work has enabled complete sampling of the two-dimensional brightness distribution of the broadened source. It is therefore possible, and of considerable interest, to compare the observed distributions to those computed on the basis of various theoretical models for the scattering process.

The simplest case to treat is that of an angular spectrum which has Gaussian cross-sections. The relation between the angular spectrum and the spatial power spectrum of the scattering irregularities is well known,[2] and the Gaussian angular spectrum we consider first is equivalent to a

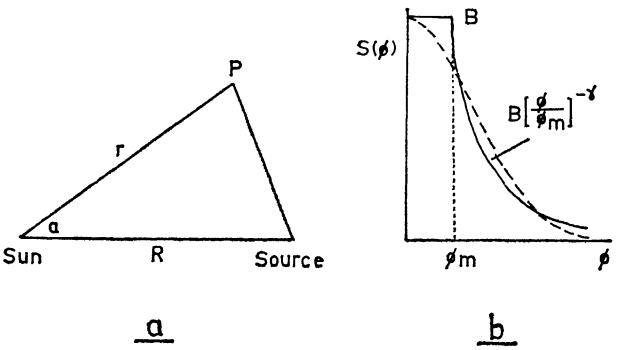

Figure 1. (a) The scattering geometry. (b) Parameters of the power-law model for the angular spectrum with a Gaussian curve shown for comparison.

Gaussian spectrum for the scattering irregularities. This model implies, therefore, a single dominant scale structure for the plasma irregularities.

In Figure 1(a) are shown the Sun and the Crab Nebula as seen projected onto the celestial sphere. It is required to calculate the brightness $B(r,\alpha)$ of all points $P(r,\alpha)$ around the true source position. We assume that the scattering gives rise to an angular spectrum of the form $\exp -(\phi^2/\phi^2_0)$, and that ϕ_0 has an elliptical distribution in the (r,α) plane with semi-axes $\phi_0(r)$ and $\phi_0(t)$ in the radial and tangential directions respectively. ϕ_0 is inversely proportional to the scale of the scattering irregularities so that, for example, radially elongated structures in the interplanetary plasma result in $\phi_0(t) > \phi_0(r)$.

Observationally it was shown in the previous paper that ϕ_0 may be represented by a power law such that

$$\phi_0(r) = \frac{r^{-S}}{A} \text{ and } \phi_0(t) = \frac{r^{-T}}{B}.$$

On this basis we can calculate the brightness of points $P(r,\alpha)$, finding the result

$$B(r,\alpha) = C/\{(A^2r^{-2S} + \theta^2)(B^2r^{-2T} + \theta^2)\}^{1/2} \times \exp -\{r^2 + R^2\cos^2\alpha - 2rR\cos\alpha) \times (A^2r^{-2S} + \theta^2)^{-1} + R^2\sin^2\alpha/(B^2r^{-2T} + \theta^2)\} \quad (1)$$

In deriving equation (1) a convolution has been performed with a source distribution $\exp -(\phi^2/\theta^2)$. For comparison with the observed brightness distributions, $B(r,\alpha)$ has been computed as a function of distance R from the Sun, and the parameter $X = A/B$. For isotropic scattering $X = 1$, and for radially elongated plasma irregularities $X > 1$. Some examples of these theoretical distributions are shown in Figure 2, where parameters have been used typical of the 1969 observations,

$$S \simeq T \simeq 2$$
$$B \simeq 1.8 \times 10^5$$
$$\theta \simeq 5.14 \times 10^{-4}$$

where all angles are expressed in radians.

In comparing such distributions with our observational data we find closest agreement using values of the elongation parameter $X = 2 - 3$. Results of such a comparison were presented at the 1970 IAU General Assembly, and we are now able to discuss the results of a more complete analysis for 1970 and 1971 data.

In Figure 3 are shown three examples of observed brightness distributions in the form of contour diagrams computed from the data recorded on magnetic tape. Beneath

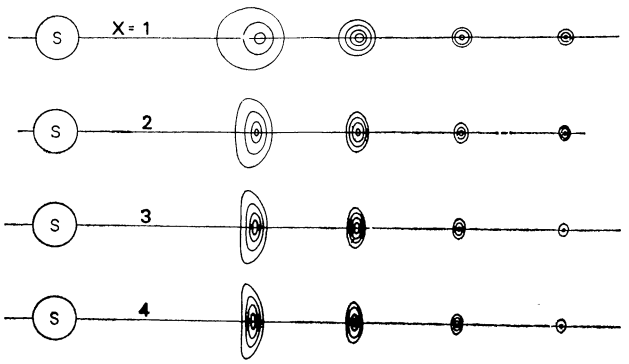

Figure 2. Theoretical brightness distributions of the Crab Nebula at various distances from the Sun, and for elongations X of the scattering irregularities.

each is the computed brightness distribution corresponding to the same radial distance from the Sun and for values of the elongation parameter $X \sim 2$. Each experimental contour plot represents an integration over at least 120 separate 1 sec. pictures, and the distribution has been deconvolved from the beam shape. Both the experimental and theoretical plots are drawn to the same linear scale in power. The close similarity between the observations and the predictions of this Gaussian model is very striking, particularly when it is considered that the region of the interplanetary medium contributing to the scattering is $\gtrsim 10^6$ km in extent for these cases. We conclude that a Gaussian form for the angular power spectrum is in remarkably close agreement with the observations, and indicates that a model of the scattering process based on a single dominant scale structure is fully able to reproduce the observations.

However, it is still conceivable that other models might also lead to satisfactory agreement with the observations and it is of interest to consider in particular the case of an angular spectrum which exhibits power-law behaviour,

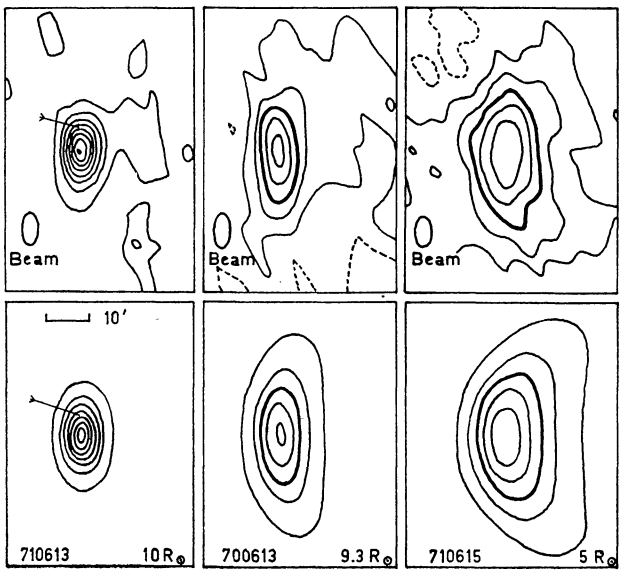

Figure 3. Observed brightness distributions compared to theoretical distributions for the same radial distances from the Sun. Heavy lines or arrows indicate the half-power contours.

and to use such a spectrum to compute the brightness distribution. Such a situation would correspond to a range of scales in the scattering medium rather than a single well-defined scale, and is in fact similar to a suggestion made recently by Jokipii and Hollweg.[3] These authors suggested a continuous spectrum of scale sizes, of turbulence form, extending from the 'inner scale' $\sim 10^6$ km detected by space vehicles, down to the 'outer' or dissipation scale $\sim$ several 100 km.

We select a power-law angular spectrum of the form sketched in Figure 1(b), with parameters chosen to give the closest fit to the observed brightness distribution after computation. The general procedure is similar to that outlined above for the Gaussian case, in that ϕ_m is taken to have elliptical form in the (r,α) plane. An example of such a calculation is shown in Figure 4, where an experimental contour plot obtained during 1971 is compared to a computed distribution assuming a Gaussian angular power

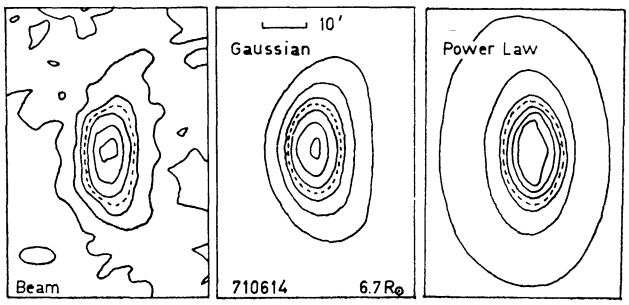

Figure 4. An observed brightness distribution compared to theoretical distributions computed for the same radial distance, on the basis of Gaussian and power-law models for the angular spectrum. The half-power contours are shown by broken lines.

spectrum, and to a distribution calculated using the power-law model with parameters chosen to give the closest fit. It is apparent that the rather 'flat-top' and initial steep slope of the power-law model do not agree with the observations. We conclude that whilst large-scale structures certainly exist in the solar wind, the present observations suggest strongly the presence of a quite distinct irregularity structure which possesses a well-defined scale at a given distance from the Sun and which is responsible for the scattering of radio waves.

In the preceding paper it was pointed out that the differing power-law indices for the radial and tangential broadening might reflect a variation of the elongation of the plasma irregularities with distance from the Sun. Values of the axial ratio of the scattered distribution obtained by fitting an elliptical Gaussian to the observed distributions using the method of least squares are shown in Figure 5. It would appear that for $r > 10\ R_\odot$, the axial ratio remains constant at $\sim 2{:}1$, a similar value to that found from spaced receiver observations of interplanetary scintillation[4] in the region $r = 70 - 200\ R_\odot$. However, our observations indicate that for $r < 10\ R_\odot$ there is a tendency for the elongation to increase to ~ 3 or 4:1 at $r \sim 5R_\odot$. It is of interest to note that this is the distance within which the magnetic pressure starts to dominate the kinetic gas pressure and where the role of the magnetic field may become more important. Indeed we might expect that the field lines within this region might deviate significantly from the radial configuration further out where the plasma pressure

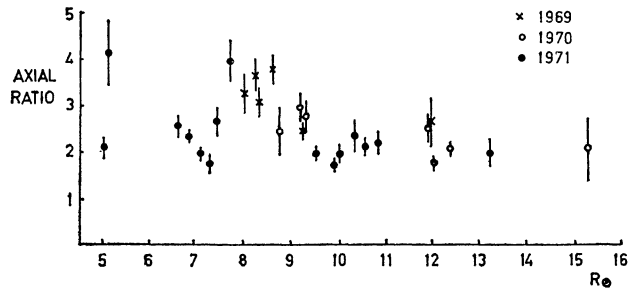

Figure 5. Values of the axial ratio of the scattered distribution as a function of radial distance from the Sun.

takes over. Our data, however, show no evidence for any deviation of the elongated irregularities (presumed elongated due to a reduction of diffusion across the field lines) from the radial direction, even to within $5R_\odot$ of the Sun. The change in axial ratio noted above may nevertheless be the first indication of the changing magnetic field configuration close to the Sun. The only previous mention of a variation in elongation was made by Slee,[5] who suggested a dependence on the phase of the solar cycle. Our results are not sufficient to examine any possible relation between the variation of axial ratio and the solar cycle.

It is a pleasure to thank the CSIRO, Division of Radiophysics, for providing observing time on the Radioheliograph. One of us (R.G.B.) acknowledges the support of a Commonwealth Postgraduate Award.

[1] Blesing, R. G. and Dennison, P. A., *Proc. ASA*, **2**, 84 (1972).
[2] Ratcliffe, J. A., *Rep. Prog. Phys.*, **19**, 188 (1956).
[3] Jokipii, J. R. and Hollweg, J. V., *Ap. J.*, **160**, 745 (1970).
[4] Dennison, P. A., *Planet. Space Sci.*, **17**, 189 (1969).
[5] Slee, O. B., *Planet. Space Sci.*, **14**, 255 (1966).

Interplanetary Scintillation Studies at the Molonglo Radio Observatory

R. G. Milne
Cornell-Sydney University Astronomy Centre, School of Physics, University of Sydney

The structure of small diameter radio sources can be investigated by studying the scintillation of the source due to the interplanetary medium when the line of sight approaches the Sun. Observations of radio source scintillation are currently being undertaken with the separate arms of the 1 mile radio telescope at the Molonglo Observatory. The EW arm allows successive transit observations with three fan beams, 1′.4 EW by 4°.2 NS at 408 MHz, bandwidth 2.5 MHz. Sources transit the half-power points of each beam in 6 sec δ seconds of time (δ is the source declination). The NS arm gives eleven fan beams at neighbouring declination, 1′.5 sec Z NS by 4° EW (Z is the zenith angle). Complete transit of a NS beam takes 15 sec δ minutes.

At each observation session sources with solar elongation $\lesssim 35°$ are selected from the Parkes and 4C catalogues and an initial survey is made using the EW arm to determine those sources that scintillate. Sources down to $\sim 1.0 \times 10^{-26}$ W m^{-2} Hz^{-1} can be observed with the EW arm. If a source shows no scintillation on two successive days for elongations $\lesssim 15°$, it is assumed to be a non-scintillator. The source will again be observed the following year. EW records can only give a qualitative idea of the strength of scintillation because of the short observation time. The total power records of the EW arm are analysed by first passing through a high pass filter to remove the aerial pattern, leaving the scintillating component which is passed through a rectifier and integrated for ~ 4 seconds. The height of the integrated signal divided by the source flux density gives a qualitative estimate of the scintillation index. Approximately 15% of all sources observed so far (~ 700) have shown significant scintillation.

Quantitative measurements of scintillation are made using the much longer transit time of the NS arm. Strongly scintillating sources are observed with two fan beams of the NS arm simultaneously, one beam 'on' the source and the other beam looking at a nearby region of sky, 'off' the source. The two beams allow correlated drifts and interference to be removed during analysis. Data are initially recorded through a 30 Hz low pass analogue filter on $\frac{1}{4}$ inch magnetic tape and later digitized at any desired sampling frequency. Approximately 4 minutes of record about transit are digitally analysed to give a scintillation index M (normalized variance of intensity), modulation power P (variance of the logarithm of intensity[2]), power spectrum, first and second moments of the power spectrum. As an example a typical NS record for the Parkes source 0518 + 16 (3C138, 17.3 f.u. at 408 MHz), at an elongation of 15°, is shown in Figure 1 and the associated power spectrum is shown in Figure 2. The 'off' source power spectrum is shown dotted.

The results obtained for 0518 + 16 are: $M \simeq 0.23$, $P \simeq 0.06$, first moment $\simeq 0.6$ Hz, second moment (square root) $\simeq 0.8$ Hz. The moments were calculated using a window in the power spectrum, 0.12 — 7.6 Hz, as discussed by Cohen *et al.*[3] However, these results should be calibrated against an 'ideal point source'. Such a source has not yet been determined. The uncalibrated results appear

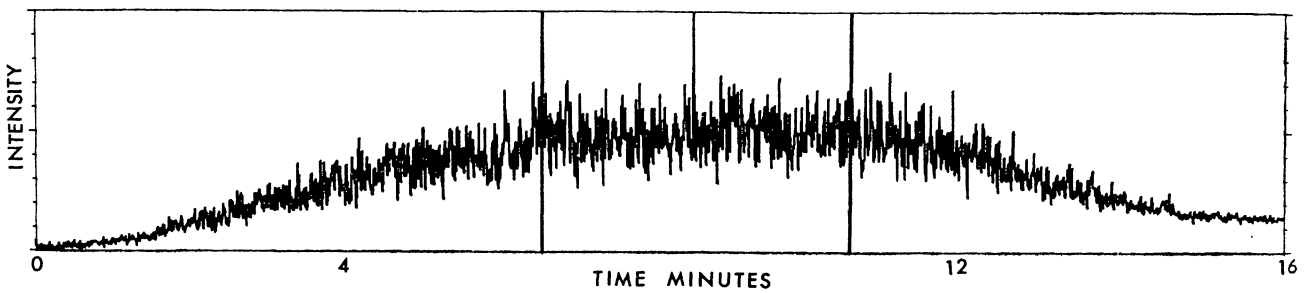

Figure 1. NS transit record for 0518 + 16. Vertical lines indicate section for digital analysis.